Microwave Landing System Requirements for STOL Operations

Stuart C. Brown,* Clifford N. Burrous,* Tsuyoshi Goka,† and Kun E. Park†
NASA Ames Research Center, Moffett Field, California

The operational/functional requirements for the new microwave landing system (MLS) are examined for STOL operations. The study utilizes a nonlinear six-degree-of-freedom simulation of a De Havilland Buffalo C-8A aircraft and automatic flight control system to assess the MLS/STOL accuracy and coverage requirements for the azimuth, DME, primary elevation, and flare elevation functions. The aircraft performance is statistically determined for representative curved flight paths through touchdown. A range of MLS errors and coverages, environmental disturbances, and navigation filtering are investigated. The filter configuration is shown to have a significant effect on the ability of the controlled aircraft to cope with the MLS navigation errors. The study indicates that the STOL MLS requirements are included within the range of proposed MLS configurations.

Downloaded by UNIVERSITY OF CALIFORNIA - DAVIS on February 9, 2015 | http://arc.aiaa.org | DOI: 10.2514/3.58644

Introduction

A PROGRAM is in progress to develop an advanced universal microwave landing system (MLS) to replace the present-day ILS.[1] The features to be included in this new system are: a common civil/military technique and signal format; modularity to satisfy the entire user spectrum; and a significant reduction in the present ILS limitations of single approach path, multipath/siting susceptibility, accuracy, capacity, and physical size. The Radio Technical Commission for Aeronautics (RTCA) Special Committee 117 has prepared a preliminary set of requirements for the MLS, and several groups[2-6] investigated the suitability of these requirements for CTOL aircraft. Similar information is required for STOL aircraft; however, a detailed assessment of the MLS requirements for STOL operations had not been performed prior to this study. The NASA Ames Research Center's STOL simulation facilities were utilized to conduct such an investigation. The MLS/STOL accuracy requirements were determined by varying the individual MLS errors and observing their effects on the aircraft dispersions at several points along the flight path, including touchdown. The MLS errors assessed include bias, random noise, and correlated noise for the MLS azimuth , elevation, and DME functions. The effects of two different sets of MLS errors also were determined, along with environmental disturbances and a range of airborne sophistication. These results are compared to tentative STOL and existing CTOL criteria, and acceptable accuracy specifications are defined.

The MLS/STOL coverage requirements were determined by varying the coverages for two representative STOL flight paths and observing the coverage needed to restabilize the aircraft after typical en route-to-MLS transitions.

System Description

This section contains a general description of the simulation equipment, the aircraft and its flight control system, the MLS navigation system and ground siting, the airborne navigation filtering the STOL flight paths, and the environmental disturbances.

The complete simulation facility of Fig. 1 consists of: a) an EAI 8400 digital computer to simulate the aircraft, Navaids (TACAN, VOR/DME, MLS) plus winds and turbulence; b) an avionics equipment rack containing the STOLAND airborne hardware, including the airborne digital computer[7]; c) a simulation cockpit with standard airborne instrumentation, together with the advanced STOLAND display and mode select system; d) and EAI 8800 analog and logic computer simulating the control surface servos and interlock logic; and e) a data conversion interface rack.

The STOLAND avionics system was developed to facilitate research in V/STOL terminal area navigation, guidance and control concepts, and hence can be operated in several levels of sophistication ranging from the manual mode with raw data displays to a fully automatic mode with time-constrained flight to touchdown. Only the fully automatic mode was used in this study, since this mode was felt to be the most demanding on MLS accuracy requirements, particularly for the higher frequency noise components. The STOLAND simulation facility contains flight certified hardware, so that the simulation can be used to validate experimental software for the STOL experiments program. Since the entire real-time data flow and system accuracies are exactly duplicated, a flight in the simulator becomes truly representative of a real flight.

The STOL aircraft simulated in this study is a prototype version of the De Havilland DHC-5 (C8-A) twin-turboprop STOL transport described in Ref. 8. The simulation model includes the six-degree-of-freedom nonlinear equations of motion; the kinematic and nonlinear aerodynamic equations; a General Electric T64-10 turboprop engine model; pitch, roll, and yaw parallel control servo models; and a simulated servo interlock unit.

The aircraft control system functions are programmed in the airborne digital computer. Generally, the sensing and frequency ranges used are comparable with present-day advanced autopilots. The MLS, DME, and EL_2 information was utilized to determine the aircraft altitude and rate from flare initiation (approximately 35 ft) to touchdown. Prior to flare initiation, normal glideslope tracking was employed. A slight amount of throttle retard was used during the exponential flare maneuver to reduce the probability of long floating touchdowns. The MLS siting geometry used for this study is shown in Fig. 2.

The MLS simulated employs a planar coordinte system and utilizes two elevation antennas (Fig. 2). The first antenna (EL_1) is used during the curved flight path and final approach phases, whereas EL_2 is used only for the flare maneuver. The aircraft position coordinates are converted into MLS signals, and the MLS error quantities are added. The MLS position signals then are converted to inertially referenced x, y, z coordinates in the airborne computer. (The z coordinate is blended

Presented as Paper 74-997 at the AIAA 6th Aircraft Design, Flight Test and Operations Meeting, Los Angeles, Calif., Aug. 12-14, 1974; submitted Aug. 13, 1974; revision received April 7, 1975.

Index categories: Aircraft Landing Dynamics; Aircraft Navigation, Communication, and Traffic Control; Instrument Landing Systems.

*Research Scientist. Member AIAA.

†National Research Council Associate.

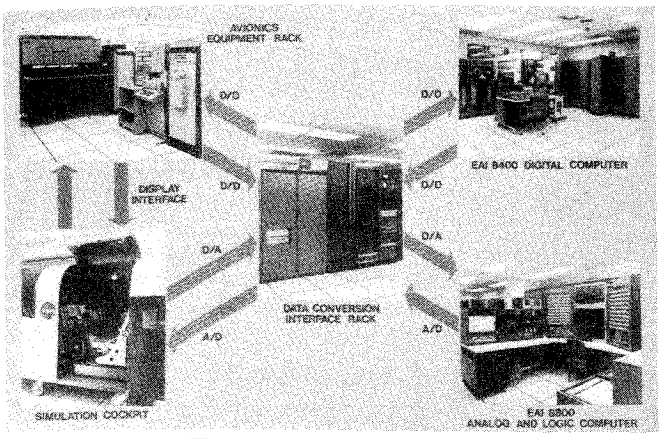

Fig. 1 Simualation facility.

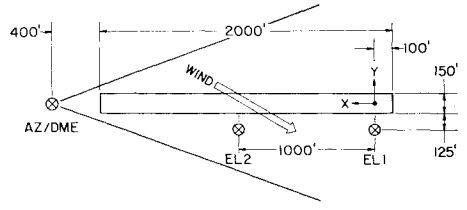

Fig. 2 STOLport MLS siting.

from the EL_1 antenna source to the EL_2 antenna between 400- and 200-ft alt.) The runway referenced x, y, and z quantities are then sent to the navigation filters along with the resolved acceleration information, and the filtered position and velocity signals are transmitted to appropriate portions of the guidance and control system.

The navigation filters employed in this study are fixed parameter complementary filters that are intended for use with a variety of navigation aids and control system modes. The filters combine resolved accelerometer information with navigation-aid derived position information given in an Earth-referenced rectangular coordinate system. The outputs are filtered position and velocity information. The horizontal channel contains three integrators, whereas the vertical channel involves two. The gains for the nominal complementary filter configuration were based on flight test experience with the STOLAND[7] system. The position signal error cutoff frequency was 0.6 rad/sec for the horizontal filter and 1.0 rad/sec for the vertical filter.

In order to investigate the effect of the navigation filter configuration on the response to MLS errors, two modifications were made to the closed-loop filters. The first modification was an increased gain complementary filter (to be called the high-frequency filter). This filter possessed about three times the bandwidth of the nominal filter for the position signal, and hence further reduced the low-frequency contribution of the acceleration signal. Hence, the effects of the MLS position errors were increased relative to the accelerometer errors. In the second modification (to be called the noncomplementary filter), the accelerometer inputs were omitted but the same order filter was maintained. The noncomplementary filter parameters were separately adjusted to give the best performance in the absence of acceleration information. The performance with such a filter is of interest, since this simplification represents a STOL aircraft with a lower avionics capability. More stringent MLS random noise specifications are required for this user, since both the position and rate information must be generated from the MLS data alone.

Two typical STOL flight paths were chosen for this study—one 90° and the other a 180° final turn (Fig. 3). The flight paths were heavily influenced by the FAA Flight Inspection Division's STOL approach procedures for ten real-life STOLports,[9] plus NASA simulation and flight experiments with curved, descending IFR STOL approaches.[10,11] Three of the ten STOLports studied in Ref. 9 required curved descending approaches, and the maximum required turn was approximately 110° with a 5000-ft radius. The straight-in final approach distance was selected to allow for glideslope tracking stabilization and the pilot's final system checks. The flight paths were flown at a constant 72-knot approach speed, so that the effects of the MLS characteristics on the longitudinal control could be monitored more readily. Figure 4 shows the atmospheric disturbance model used for this simulation. The wind direction was 30° with respect to the runway, as shown in Fig. 2.

Results and Discussion

Simulation Conditions and Criteria

All data were taken with the following conditions (except for parts of the coverage section as noted): 1) 6° glide slope; 2) flight path 1; 3) initialization at $Y = -20{,}000$ ft with stability achieved prior to WP 3; 4) all runs included the wind described in Figs. 2 and 4; 5) the turbulence of Fig. 4 was added only where indicated; 6) MLS coverage limits of ±60° horizontal and 20° vertical; 7) MLS data rate = 5.0 Hz, except $EL_2 = 10.0$ Hz; 8) STOLAND operation in the automatic II mode (synonymous to autoland); 9) 10 runs for all random errors; 10) MLS resolutions were ±4 ft for DME and ± 0.003° for azimuth and elevation angles; 11) All dispersions are plotted with $\pm 1\sigma$ dimensions.

Figure 5 shows the two sets of MLS (bias and random) error combinations which were utilized in this study. The first set, to be called combination A, was established by converting the RTCA[12] CAT III MLS touchdown displacement errors to angular errors for the STOLport MLS siting shown in Fig. 2. These angles became significantly larger than those shown in the RTCA document, because the STOLport is 1/7 the length of the RTCA 14,000-ft CTOL runway. The second set, to be called combination B MLS errors, was not derived from RTCA, but reflects an increase of 2 to 5 over the combination A errors. These random and bias errors are intended to represent the total ground transmitter and the airborne receiver errors.

One of the most difficult parts of this task is the comparison of the simulation results to known STOL criteria. There are no FAA or ICAO specifications for any category of STOL touchdown or decision height dispersions. In lieu of such standards, the results are compared to the existing FAA CTOL aircraft standards of Fig. 6.[13,14] The criterion given for the CTOL decision height standards of Fig. 6 refers to deviations obtained from indicated angular errors. However, for the purpose of evaluating MLS guidance errors, a performance criterion based on aircraft flight path errors is more meaningful. This distinction is particularly significant for bias effects, since such errors would not be apparent with an indicated error criterion. Figure 6 also shows a tentative STOL touchdown criterion. One of the objectives of the STOL operating experiments program is to develop a data base for establishing such criteria. Note that the criteria shown in Fig. 6 are given as 2σ values. With the number of parameters to be investigated in this study, it was not feasible to make a sufficient number of statistical runs to obtain this level of accuracy. However, the limited number of runs made is sufficient to indicate the primary effects of MLS parameter changes.

Accuracy

Individual MLS Errors

The effects of the individual bias, random and correlated MLS errors were evaluated with the nominal airborne com-

Downloaded by UNIVERSITY OF CALIFORNIA - DAVIS on February 9, 2015 | http://arc.aiaa.org | DOI: 10.2514/3.58644

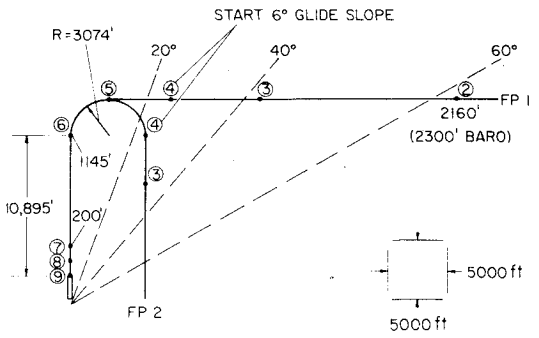

Fig. 3 Flight paths.

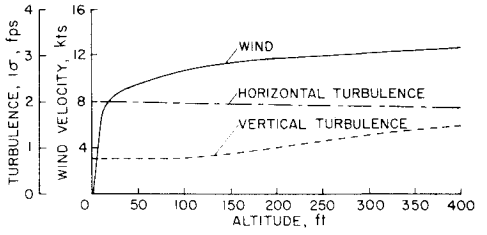

Fig. 4 Atmospheric disturbance model.

ERROR COMBINATION	FUNCTION	UNITS	BIAS (1σ)	RANDOM (1σ)
A FROM RTCA SC-117 CAT III SPEC FOR STOLPORT	Az	deg	0.124	0.112
	EL_1	deg	.036	.042
	EL_2	deg	.034	.032
	DME	ft	20	20
B	Az	deg	0.3	0.2
	EL_1	deg	.1	.15
	EL_2	deg	.1	.15
	DME	ft	100	100

Fig. 5 MLS error combinations.

A. FAA AUTO LANDING SYSTEM ADVISORY CIRCULAR 20-57A FOR CAT II CTOL

- 2σ LONGITUDINAL TOUCHDOWN DISPERSION = <1500 ft TOTAL (NEED NOT BE SYMMETRICAL).
- 2σ LATERAL TOUCHDOWN DISPERSION = < ± 27 ft ABOUT R/W CENTERLINE.

ATTEMPTING TO SCALE THESE FIGURES TO A STOLPORT GIVES:

- 2σ LONGITUDINAL STOL TOUCHDOWN DISPERSION = < 700 ft TOTAL.
- 2σ LATERAL STOL TOUCHDOWN DISPERSION = <±24 ft OF CENTERLINE

B. FAA CRITERIA FOR APPROVAL OF CAT II LANDING WEATHER MINIMA ADVISORY CIRCULAR AC 120-29 FOR ILS/CTOL 100 ft DECISION HEIGHT WINDOW.

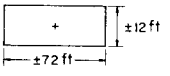

THE VALUES GIVEN FOR THIS WINDOW ARE INTERPRETED TO MEAN THAT THE AIRCRAFT SHOULD BE WITHIN THE SPECIFIED LIMITS FOR AT LEAST 95% OF THE APPROACHES ATTEMPTED. WITH THE ASSUMPTION OF A GAUSSIAN DISTRIBUTION, THE RESULTING VERTICAL AND HORIZONTAL 2σ ERRORS BECOME ±12 ft AND ±72 ft, RESPECTIVELY.

Fig. 6 Criteria.

plementary filter discussed in the section headed System Description.

Bias Errors

Each bias error was evaluated separately, except that equal values of EL_1 and EL_2 errors were varied simultaneously. During the assessment of each MLS bias error, all other bias errors were held at the low positive 1σ combination A levels defined in Fig. 5, and the random noises were reduced to ¼ of the combination A magnitudes.

It is difficult to assess accurately an acceptable magnitude of an individual MLS error without knowing the contribution of other error sources that affect the total dispersion of interest. However, since it is impossible to study all of the potential combinations of MLS errors, these individual error cases allow extrapolations from the combination error data. The effects of MLS bias errors on dispersions at touchdown and at 100 ft alt are shown in Figs. 7 and 8, respectively. The influence of azimuth bias on lateral dispersions and of elevation and DME biases on longitudinal and vertical dispersions are indicated.

Azimuth Bias

Figure 7 shows the effect of azimuth bias on lateral touchdown dispersion. The aircraft lateral touchdown points are in fair agreement with the calculated signal errors, although they are biased a few feet in the negative direction because of the wind effects and the resulting decrab maneuver. The 0.4° MLS azimuth bias is clearly unacceptable, because it alone results in lateral errors that exceed the ±12 ft (1σ) STOL criteria of Fig. 6.

Figure 8 shows the effect of azimuth bias on aircraft lateral position at 100 ft alt. The aircraft is wihin the CTOL ±36 ft (1σ) lateral window, even with 0.4° of azimuth bias; however, this value is too large to allow for reasonable levels of random azimuth noise, horizontal turbulence, etc.

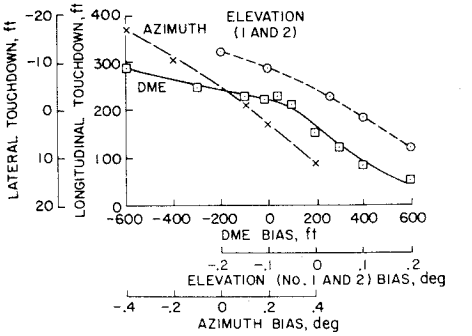

Fig. 7 Effects of MLS biases on touchdown locations.

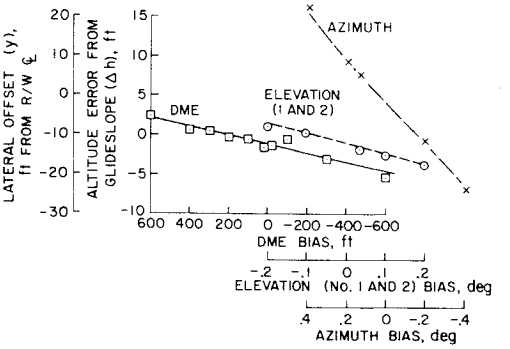
LATERAL OFFSET (y), ft FROM R/W ℄
ALTITUDE ERROR FROM GLIDESLOPE (Δh), ft
AZIMUTH
ELEVATION (1 AND 2)
DME
DME BIAS, ft
ELEVATION (NO. 1 AND 2) BIAS, deg
AZIMUTH BIAS, deg

Fig. 8 Effects of MLS biases at 100-ft alt.

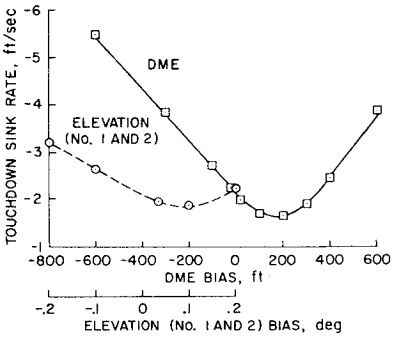

Fig. 9 Effects of MLS biases on touchdown sink rate.

Downloaded by UNIVERSITY OF CALIFORNIA - DAVIS on February 9, 2015 | http://arc.aiaa.org | DOI: 10.2514/3.58644

Downloaded by UNIVERSITY OF CALIFORNIA - DAVIS on February 9, 2015 | http://arc.aiaa.org | DOI: 10.2514/3.58644

Elevation Bias

The effects of EL_1 and EL_2 biases on longitudinal touchdown dispersion also are shown in Fig. 7, whereas the effect on touchdown sink rate is inlcuded in Fig. 9. (Equal EL_1 and EL_2 error magnitudes were chosen in order to obtain the effect of a single magnitude for all points along the trajectory. For the control law sequence employed, the EL_1 signal is primarily used prior to the 35-ft flare initiation height, whereas the EL_2 signal is used from that point to touchdown.) The $\pm 0.2°$ elevation bias results in approximately 200 ft (total) of longitudinal dispersion, which is unacceptable for this single error source. The effect of elevation bias errors on touchdown sink rate is not significant below $\pm 0.2°$.

Figure 8 shows the effect of the same elevation biases at the 100-ft alt. The $\pm 0.2°$ biases produce approximately one-half of the allowable ± 6 ft vertical dispersion of Fig. 6, and hence, are slightly high to allow for reasonable levels of EL_1 and EL_2 random noise and turbulence.

DME Bias

The magnitude of DME errors that can be tolerated depends on the manner in which the DME information is utilized by the control system. That is, are the DME and elevation angle data used to calculate altitude in place of a radio altimeter, and during what portion of the flight path does this occur? As discussed in the System Description section, this simulation employed glideslope tracking until flare initiation, and then utilized DME and EL_2 data to calculate altitude during flare.

The effects of DME bias on longitudinal touchdown dispersions are shown in Fig. 7, and the resulting touchdown sink rates are demonstrated in Fig. 9. A comparison of these two figures shows that the limiting factor for DME bias is the touchdown sink rate.

Figure 8 shows the effect of DME bias on altitude errors at 100-ft alt. Reasonable levels of DME bias have a relatively small effect on vertical dispersions because glideslope tracking is employed at this point. Large DME bias errors can be tolerated if the transition to radio altimeter and/or manual flare is made at 100 ft and the other MLS errors which affect

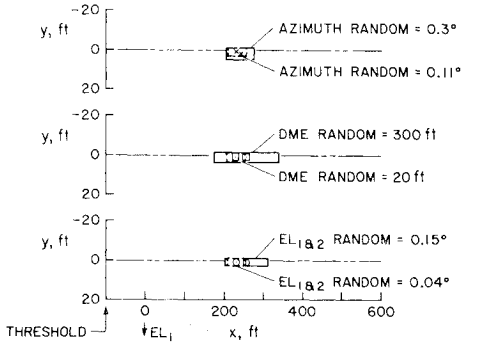

Fig. 10 Effects of MLS random noise on touchdown dispersions.

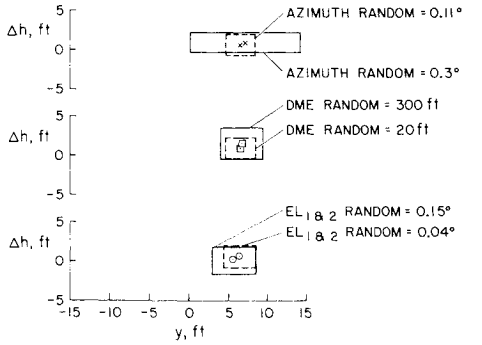

Fig. 11 Effects of MLS random noise at 100-ft alt.

Δh are kept to a minimum. However, the STOL 100-ft and flare initiation altitudes are reached (longitudinally) before the runway surface. Therefore, terrain irregularities may preclude the use of radio altimeters at many STOLports. The entire DME accuracy subject must be further analyzed in the light of the recent interest in L-band DME for MLS, and the projected increase in DME cost if the total DME errors must be less than approximately 100 ft.

Random Noise

The effects of the individual MLS random errors were assessed with the nominal vertical and horizontal complementary filtering. All of the individual random error runs include the combination A fixed-positive 1σ bias and random noise background on all functions. Hence, the smaller dispersions in Figs. 10 and 11 represent the dispersions due to the combination A MLS errors, as well as the particular error under study. (A small percentage of these dispersions is attributable to the STOLAND and interface hardware.) All data were taken with the wind described in Figs. 2 and 4.

Azimuth Random Noise

Figure 10 shows the effect of azimuth random noise on lateral touchdown dispersion. Notice that the system with complementary filtering results in aircraft dispersions that are approximately ½ of the corresponding azimuth random signal errors. The mean lateral touchdown point is shifted slightly and the lateral dispersion is increased 30% as the azimuth random noise is increased from 0.11° to 0.3°. The lateral touchdown dispersion caused by the 0.3° random azimuth noise is too large to allow for reasonable values of azimuth bias, crosswinds, and turbulence. Figure 11 illustrates the effect of random azimuth noize on lateral dispersion at the 100-ft alt. The 0.3° random noise increases the lateral dispersion by a factor of 3.5, but is still well within the ± 36 ft (1σ) CTOL specification.

DME Random Noise

The effects of 20- and 300-ft DME random noise at touchdown and 100-ft alt are compared in Figs. 10 and 11, respectively. The 160-ft longitudinal touchdown dispersion caused by the 300-ft DME random noise is excessive. At 100-ft alt, the 300-ft DME random noise causes a relatively small increase in vertical dispersion.

Elevation Random Noise

Figures 10 and 11 also show the effect of EL_1 and EL_2 random errors on the touchdown and 100-ft-alt dispersions. At large distances from the EL_1 antenna, a significant increase in h, Δh, and forward velocity oscillations are observed when the EL_1 random noise is increased from 0.042° to 0.15°. Since 0.15° of EL_2 random noise shifts the mean touchdown point approximately 30 ft and more than doubles the longitudinal dispersion, 0.1° is probably a more acceptable value. The 0.15° EL_1 and EL_2 random noise has very little effect on the Δh dispersions at 100-ft alt.

Combination Random Bias and Noise (without Turbulence)

Figures 12 and 13 compare the effects of combination A and B MLS *random bias* and noise at touchdown and 100-ft alt. Figure 12 shows that the combination B azimuth errors are excessive because the lateral touchdown dispersions exceed the ± 12 ft (1σ) tentative STOL criteria, even without turbulence or random crosswinds. The combination A azimuth errors are well within limits, and it appears that a value between the combination A and B azimuth errors would be acceptable. The longitudinal touchdown dispersions, and hence the related combination B DME and elevation errors, are within the criteria and still should be acceptable when allowance is made for other factors, such as turbulence.

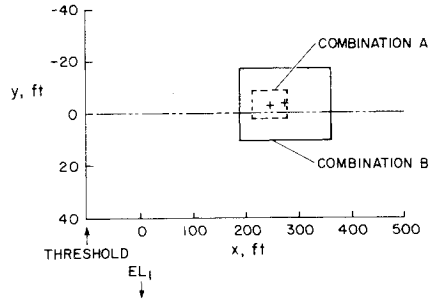

Fig. 12 Comparison of touchdown dispersions with combination A and B MLS random bias and noise (without turbulence).

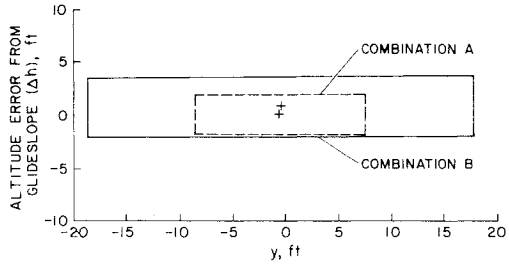

Fig. 13 Comparison of dispersions at 100-ft alt with combination A and B MLS random bias and noise (without turbulence).

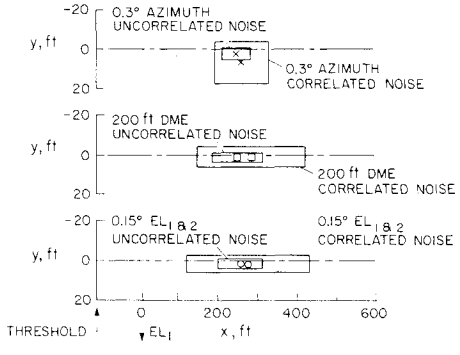

Fig. 14 Comparison of the effects of correlated (2-sec time constant) and uncorrelated MLS noise at touchdown.

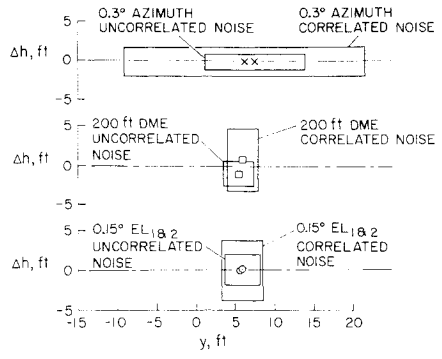

Fig. 15 Comparison of the effects of correlated (2-sec time constant) and uncorrelated MLS noise at 100-ft alt.

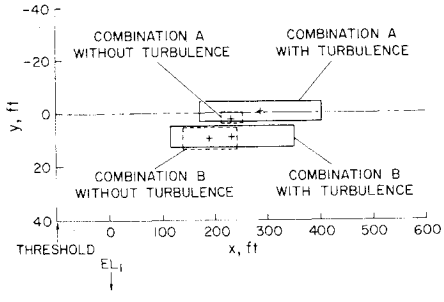

Fig. 16 Comparison of touchdown dispersions with combination A and B MLS fixed bias and random noise errors (with and without turbulence).

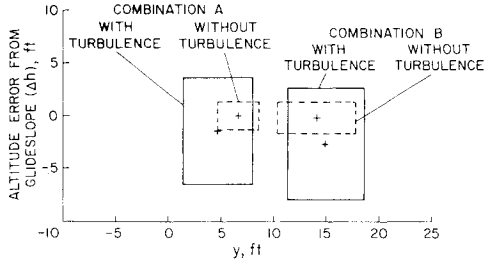

Fig. 17 Comparison of dispersions at 100-ft alt with combination A and B MLS fixed bias and random noise errors (with and without turbulence).

Figure 13 indicates that the 100-ft-alt lateral and vertical dispersions that result from the combination B errors are within the CTOL ± 36 and ± 6 ft (1σ) criteria, respectively.

Correlated Noise

Although the preliminary MLS accuracy specifications[12] refer only to uncorrelated random noise, subsequent specifications further define the frequency content and allow for correlated noise. A principal source of this noise is multipath effects, although other sources also may produce correlated noise at the airborne receiver output. No attempt was made to assess the magnitude of these potential correlated noise sources. Instead, noise parameters were varied selectively to provide information on the magnitudes necessary to cause interference with aircraft tracking performance.

Comparisons are made of the effects of correlated (2-sec time constant) and uncorrelated MLS random noise at touchdown and the 100-ft alt (Figs. 14 and 15). All MLS errors were the combination A positive fixed bias and random noise levels, except for the particular quantity indicated in the figure. The nominal complementary filters and wind were included.

The correlated noise has a significant effect on touchdown dispersions. For instance, the lateral dispersion due to the correlated azimuth noise is three times higher than that resulting from the same magnitude of uncorrelated noise. At the 100-ft alt, similar trends occur. The lateral dispersions due to azimuth correlated noise, and the vertical dispersions due to the DME and elevation correlated noise, all are increased by a factor of two.

Although not shown, time histories demonstrate that these correlated noises deteriorate parameters in other portions of the flight path. The correlated azimuth noise causes a 2-to-1 increase in the lateral position, lateral acceleration, and heading angle oscillations over the entire flight path. The correlated DME noise results in relatively large lateral oscillations and control motions prior to the final 90° turn. Although the effects of the correlated elevation noise were relatively small for the final portion of the approach, significant vertical oscillations and airspeed changes occurred prior to the final turn.

The presence of correlated noise in the MLS signals results in a significant increase in a number of the aircraft dispersions. These changes demonstrate the need for detection of such noise sources in the MLS hardware and for the inclusion of frequency, as well as magnitude, criteria in future MLS accuracy specifications.

Downloaded by UNIVERSITY OF CALIFORNIA - DAVIS on February 9, 2015 | http://arc.aiaa.org | DOI: 10.2514/3.58644

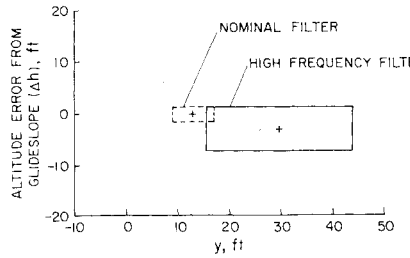

Fig. 18 Effect of complementary filter cutoff frequency on dispersions at 100-ft alt (combination B fixed bias and random noise errors).

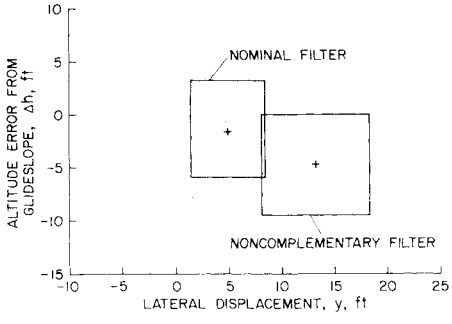

Fig. 19 Effect of noncomplementary filter on dispersions at 100-ft alt (combination A fixed bias and random noise, with turbulence).

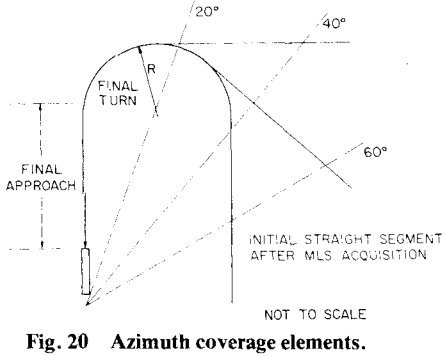

Fig. 20 Azimuth coverage elements.

MLS Error Combinations with Turbulence

This section contains results for the combination A and B MLS errors with and without turbulence. The nominal complementary navigation filters were utilized, and the previously described wind and turbulence were included. The fixed positive 1σ biases of Fig. 5 were used in order to separate the effects of MLS bias and random errors (The dashed dispersions of Figs. 16 and 17 represent standard deviations due to the MLS random noises only since the MLS biases are fixed at the positive 1σ values.) The effects of turbulence (Figs. 16 and 17) also will be compared to the combined MLS errors in Figs. 12 and 13.

The aircraft dispersions at touchdown are summarized in Fig. 16. Without turbulence, the standard deviations due to the combination B errors are at least twice those due to the combination A errors. Comparing Figs. 12 and 16 shows that the addition of turbulence increases the longitudinal touchdown dispersions by a factor of 1.5 to 3.5 for the combinations B and A MLS errors, respectively. Although not shown, the touchdown sink rate is increased only slightly in the presence of turbulence. The mean and standard deviation only rise to about 2.3 and 0.5 fps, respectively, and hence are quite acceptable. Note that the 1σ touchdown dispersion pattern is almost the same for both MLS error combinations with turbulence, although the means are shifted as indicated (Fig. 16). Both sets of longitudinal touchdown dispersions are approximately 2/3 of the STOL criteria, and the means appear to be acceptable. A comparison of Figs. 12 and 16 indicate that, for the range of values shown, the random azimuth bias errors have a greater effect on lateral touchdown dispersions than turbulence. Comparing estimates of the total lateral touchdown dispersion to the STOL criteria shows that the combination B lateral dispersions exceed the ± 12 ft (1σ) from centerline STOL criteria; hence, the 0.3° azimuth bias is excessive.

The glideslope tracking errors at 100-ft alt are shown in Fig. 17. Without turbulence, the increased combination B random errors do not affect the vertical standard deviation appreciably whereas the lateral value is doubled. A comparison of Figs. 13 and 17 shows that the vertical dispersions are significantly increased by the addition of turbulence. Note that the vertical dispersions with either combination are so close to the CTOL ± 6 ft (1σ) criterion that no allowance is available for other factors, and reducing the MLS errors would not improve the situation significantly. The lateral standard deviations with turbulence are approximately the same for both combinations (Fig. 17). However, a comparison of Figs. 13 and 17 indicates that the azimuth random bias has the major effect on lateral dispersions. Note that the total lateral dispersions due to turbulence are approximately the same for both combinations (Fig. 17). However, a comparison of Figs. 13 and 17 indicates that the azimuth random bias has the major effect on lateral dispersions. Note that the total lateral dispersions due to turbulence and MLS errors still should be below the CTOL ± 36 ft (1σ) criterion.

Figures 16 and 17 show that several of the STOL aircraft dispersions are significantly increased by turbulence, and hence the turbulence defines a lower limit for these dispersions. This is not surprising since most STOL aircraft have no more than medium wing loadings and fly at relatively slow approach speeds (60-80 knots), and thus are generally more susceptible to environmental disturbances than CTOL aircraft.

Complementary Filter Variations

The complementary filter characteristics were described in the System Description section. This section will show the changes in aircraft response which result from an increase in the position error cutoff frequency of the horizontal and vertical filters. The filter gains for both the horizontal and vertical filters were adjusted to increase the filter breakpoint frequencies by a factor of 3, while the frequency response shape for position errors was maintained. The design of a complementary filter involves tradeoffs between filtering to attenuate the high-frequency portion of the position signal relative to the low-frequency portion of the acceleration signal. Increasing the filter gains (increase in position error cutoff frequency) results in a deterioration of the position error filtering while improving the low-frequency acceleration filtering. Hence, the increased gain setting represents a filter adjustment that relies more on the MLS position information and is indicative of the compromise needed to further reduce the effects of acceleration errors associated with a minimum cost accelerometer installation.

Comparisons of dispersions for the nominal and high-frequency filters at 100-ft alt are shown in Fig. 18. The previously described combination B random and fixed positive bias errors were used together with the nominal wind disturbance. The errors for the high-frequency filter are seen to be much larger than those for the nominal filter, and similar results occurred for other points along the trajectory. Both the lateral and vertical errors for the high-frequency filter exceed the CTOL criteria of Fig. 6. (Time histories also indicate a substantial increase in control surface motion.) Hence, the high-frequency filter is not considered to provide adequate performance with this random noise level.

Downloaded by UNIVERSITY OF CALIFORNIA - DAVIS on February 9, 2015 | http://arc.aiaa.org | DOI: 10.2514/3.58644

Table 1 Summary of the microwave landing system requirements for STOL operations

MLS function		MLS requirements for STOL operations with complementary filtering	MLS requirements for STOL operations without complementary filtering	RTCA SC-117 specifications Configuration D	RTCA SC-117 specifications Configuration I
Accuracy (1σ)					
azimuth	Bias	0.15°	0.15°	0.14°[a] (0.37°)[b]	0.02°[1] (0.12°)[b]
	Noise	0.15°	0.1°	0.07° (0.18°)	0.02° (0.11°)
elevation no. 1	Bias	0.1°	0.1°	0.04° (0.12°)	0.04° (0.04°)
	Noise	0.1°	0.04°	0.05° (0.13°)	0.05° (0.04°)
elevation no. 2	Bias	0.07°	---	---	0.02° (0.03°)
	Noise	0.08°	---	---	0.02° (0.03°)
DME	Bias	100 ft	100 ft	300 ft	20 ft
	Noise	100 ft	40 ft		
Coverage					
horizontal		±45°	±45°	±20°	±40°
maximum vertical		20°	20°	8° Hz and DME	
range		10 nm	10nm	20 nm	20 nm
Data rate		5 Hz all but EL_2@10 Hz	5 Hz	5 Hz	5 Hz all but EL_2@10 Hz

[a] Specifications based on CTOL aircraft siting. [b] Specifications based on STOLport siting.

Downloaded by UNIVERSITY OF CALIFORNIA - DAVIS on February 9, 2015 | http://arc.aiaa.org | DOI: 10.2514/3.58644

Noncomplementary Filter

As described in a previous section, the vertical and horizontal navigation filter gains also were adjusted for optimum performance without acceleration signals. The lateral control gains also were reduced from the normal values in order to improve stability and reduce the control surface activity in the presence of measurement noise. Runs were made with the combination A MLS random and fixed positive bias errors with the standard wind and turbulence.

The flare and touchdown performance was not satisfactory because the aircraft dynamics were too rapid for the vertical filter to provide useable estimates for the control system. Therefore, for automatic landing from a 6° flide slope, vertical acceleration information is required for flare and touchdown.

The final approach capture and tracking performance with the noncomplementary filter was somewhat deteriorated from the complementary filter case. Although not shown, the average lateral overshoot of the runway centerline was about 200 ft, whereas the overshoot was negligible for the complementary filter case. The vertical tracking performance was comparable except for a slightly greater overshoot at the glideslope initiation. Moreover, time histories showed that the accelerations and control motions during the capture and tracking phase were acceptable with the combination A MLS errors.

The 100-ft-alt dispersions with both filters are compared in Fig. 19. The lateral and vertical standard deviations with the noncomplementary filter are within the CTOL criteria; however, the vertical mean is low. These results indicate that the noncomplementary filter system can capture and track the flight path no. 1 final approach in the presence of the combination A random errors. Additional preliminary data have indicated that satisfactory performance still may be achieved in the presence of somewhat higher MLS errors if the filter and control gains are lowered and the flight-path maneuver requirements are reduced. That is, increase the final approach length and the turn radius, and decrease the glideslope transition angle.

MLS Coverage Requirements

Figure 20 illustrates the three basic flight path elements that determine the azimuth horizontal coverage requirements. These include a minimum straight-in final approach, final turn radius, and an initial straight segment after MLS acquisition and prior to any major maneuver. Many factors influence the dimensions of these elements; however, one can see that the azimuth horizontal coverage requirement increases if: 1) the final turn radius is increased; 2) the final approach distance is decreased; or 3) the initial approach angle is increased.

The MLS must provide vertical coverage above the potential 6° and 10° STOL glideslope angles, plus a reasonable margin to allow for altimeter errors and MLS vertical coverage prior to descent. The two flight paths used to evaluate coverage are shown in Fig. 3 and discussed in the System Description section. The criteria used in determining the MLS/STOL coverage requirements was that the aircraft be reasonably stabilized after the en-route-to-MLS transition before any subsequent maneuver, such as glideslope descent or the start of the final turn.

In order to simulate typical en route-to-MLS transition errors for a TACAN station near the STOLport, the following TACAN errors were included: DME bias = +1000 ft, DME random noise = 172 ft (1σ), and bearing bias = +1.5°. The MLS errors were the combination A fixed bias and random noise levels. The azimuth and elevation vertical coverages were 20°, and the horizontal coverage was varied as indicated. The airborne system was configured to operate with horizontal MLS information when the azimuth and DME signals are valid, or with both horizontal and vertical MLS information when the azimuth, DME, and elevation signals are valid. The coverage assessment for each flight path is as follows.

Flight Path No. 1 (90° Final Turn)

Figure 21 shows several aircraft state parameters over the region of the TACAN/MLS transition through the start of the 6° glideslope descent. The data on the left show that for an azimuth horizontal coverage of ±60° the aircraft has had adequate time to stabilize after the TACAN/MLS transition prior to the glideslope descent at waypoint 4. However, the right-hand side of Fig. 21 shows that reducing the azimuth horizontal coverage to ±40° leaves just enough time for the aircraft state quantities to stabilize prior to waypoint 4 (50 sec and 6000 ft). The aircraft made a successful autoland in both cases; however, pilots generally prefer to be stabilized prior to the first maneuver within coverage. On this basis ±40° is probably the absolute minimum azimuth horizontal coverage for flight path no. 1. In order to provide some allowance for more stringent en route navigation aid locations and errors, ±45° is preferred. For navigation aids located at 20 to 30 naut. mile distances from the MLS boundary, some modification of the flight path probably would be required in order to allow sufficient time to restabilize. Waypoint 4 is at an azimuth vertical angle of 8°; hence, an azimuth vertical coverage of approximately 10° is satisfactory for this flight path.

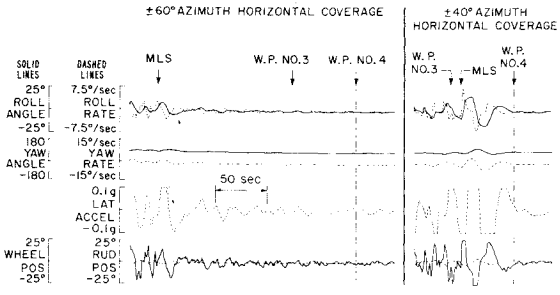

Fig. 21 Comparison of aircraft stability at the initial descent point (waypoint 4) with ±60° and ±40° azimuth horizontal coverage, flight path no. 1.

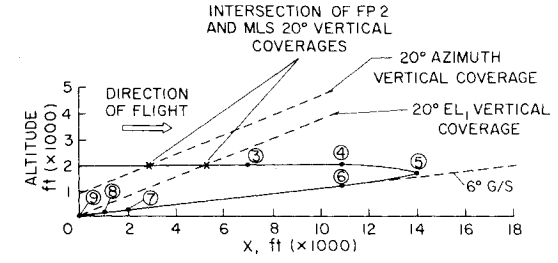
INTERSECTION OF FP 2 AND MLS 20° VERTICAL COVERAGES
20° AZIMUTH VERTICAL COVERAGE
DIRECTION OF FLIGHT
20° EL1 VERTICAL COVERAGE
ALTITUDE ft (×1000)
6° G/S
X, ft (×1000)

Fig. 22 Flight path profile showing the intersection of flight path no. 2 and the MLS 20° vertical coverages

Vertical transitions from TACAN to MLS coverage were performed with a 125-ft-alt error in the TACAN coverage area. Although not shown, the pitch angle, flight-path angle, $\dot{h}$, and elevator parameters all are restabilized within approximately 30 sec or 3500 ft. Hence, with ±60° of EL_1 horizontal coverage, the aircraft is vertically stable long before the start of glideslope descent at waypoint 4. With ±40° of EL_1 horizontal coverage the aircraft has barely stabilized in the vertical and longitudinal axes prior to waypoint 4. The elevation vertical angle at waypoint 4 is 9°, and so at least 10° of EL_1 vertical coverage is required.

Flight Path No. 2 (180° Final Turn)

Although not shown, simulations were made with flight path no. 2 with the same conditions as previously described for flight path no. 1. Figure 22 demonstrates the increased vertical coverage requirements for flight path no. 2. Notice that this flight path does not fall within the 20° EL_1 vertical coverage until approximately 5400 ft before the start of glideslope descent, whereas flight path no. 1 is easily covered by an EL_1 vertical coverage slightly greater than 9°. Flight path no. 2 (Figs. 3 and 22) also demonstrates the need to utilize azimuth/DME information as soon as it is available independent of the availability of vertical information.

Considering the path length requirements for completing the lateral and vertical transitions of flight path no. 1, the minimum MLS coverage requirements for flight path no. 2 are as follows. the azimuth/DME horizontal and vertical angle associated with the 6000-ft lateral transition requirement are 42° and 17°, respectively. Therefore, coverages of 45° and 20°, respectively, are needed to provide an operating margin. Similarly, the vertical transition characteristics result in an EL_1 horizontal and vertical coverage requirement of ±40° and 20°, respectively.

Summary of the MLS Specifications for STOL Operations

The selection of the level of MLS errors that can be tolerated, in combination with all of the other error sources, is difficult because the study could only assess a limited number of variables. That is, it was limited by the range of airborne sophistication, statistics, siting, flight paths, atmospheric disturbances, and a single aircraft. Furthermore, the STOL decision heights, windows, and touchdown criteria still are under development. However, even with the uncertainties, it appears that the MLS errors listed in Table 1 can be tolerated in STOL terminal area operations. Two sets of category II/III accuracy requirements are listed in Table 1: 1) a set for aircraft equipped with an autoland system with an inertially augmented navigation capability, and 2) a set for aircraft equipped for automatic final approach tracking but without complementary filtering. The main difference between the two sets is more stringent noise requirements for the case without complementary filtering. Although not investigated, additional filtering of the DME signal for the system without complementary filtering may be feasible with satisfactory tracking performance still maintained; hence, the value of DME noise given in Table 1 for this system may be conservative. For comparison, the RTCA SC-117 preliminary recommendations[12] for a category I and III MLS are shown. (The linear RTCA accuracy specifications have been converted to angular dimensions using typical CTOL runway lengths and MLS sitings. The angles in parenthesis are based on the STOLport siting of Fig. 2.)

The MLS coverage and data rate requirements also are summarized in Table 1. The coverage requirements were determined from the two STOL flight paths and en route/MLS sitings and errors evaluated in the report. The 5.0 Hz data rate for all functions except EL_2 (at 10 Hz) used in the analysis appears to be adequate for the flight paths and range of errors evaluated. The characteristics of STOL air transportation operations are felt to require only a 10-naut. mile range rather than the proposed 20-naut.-mile value.

Conclusions

Table 1 summarizes the MLS accuracy, coverage, and data requirements for the STOL operations evaluated in this report. Comparing the STOL specifications to the RTCA configurations[12] shows that the RTCA D configuration (intended for a longer CTOL runway) satisfies all of the STOL accuracy requirements with the exception of DME (and EL_2 for CAT III). The I configuration satisfies all of the STOL requirements except for a small difference in horizontal coverage.

The levels of turbulence assessed in this report have a significant effect on longitudinal touchdown dispersions and vertical dispersions at 100-ft alt. The addition of turbulence to the overall combination A MLS error causes these two dispersions to increase by a factor of approximately three. Decreasing the MLS accuracy specifications below the combination A values would not reduce the dispersions significantly in the presence of turbulence, since there is a minimum performance limit based on the controlled aircraft's ability to cope with the environment distrubances.

Correlated MLS noise (with a 2-sec time constant) increases the dispersions at touchdown and 100 ft alt by a factor of at least two as compared to the same magnitude of uncorrelated noise. Hence, frequency content, as well as magnitude, must be included in the MLS noise specifications.

The noncomplementary filter configuration successfully captured and tracked the final approach in both the horizontal and vertical channels with the lower combination A MLS errors. The flare maneuver was not satisfactory without measured vertical acceleration information.

References

[1] Anon., "National Plan for Development of the Microwave Landing System," DOT-NASA-DOD, AD 733268, July 1971.

[2] Lanman, M., H., "An Investigation of Microwave Landing Guidance System Signal Requirements for Conventionally Equipped Civilian Aircraft," RD-71-86, Federal Aviation Agency, Washington, D.C., June 1971.

Downloaded by UNIVERSITY OF CALIFORNIA - DAVIS on February 9, 2015 | http://arc.aiaa.org | DOI: 10.2514/3.58644

[3]Lanman, M. H., "Microwave Landing System Signal Requirements for Conventional Aircraft," Federal Aviation Agency, Washington, D.C., RD-72-86, July 1972.

[4]Hofmann, L. G., Clement, W. F., Graham, D., Blodgett, R. E., and Shah, K. V., "Investigation of Measuring System Requirements for Low Visibility Landing," TR-71-151, Air Force Flight Dyanmics Lab., Wright-Patterson Air Force Base, Ohio, Dec. 1971.

[5]Dillow, J. D., Stolz, P. R., and Zuckerman, M. D., "Analysis of Data Rate Requirements for Low Visibility Approach with a Scanning Beam Landing Guidance System," TR-71-177, Air Force Flight Dynamics Lab., Wright-Patterson Air Force Base, Ohio, Feb. 1973.

[6]Benjamin, J., "A Review of Approach and Landing Guidance in Relation to Civil and Military Requirements," TR 71186, Royal Aircraft Establishment, Farnsborough, England, Sept. 1971.

[7]Young, L. S., Hansen, Q. M., Rouse, W. E., and Osder, S. S., "Development of STOLAND, a Versatile Navigation, Guidance, and Control system," TM X-62,183, NASA, 1972.

[8]Taylor, J. W. R. (ed.), *Jane's All the World's Aircraft 1968-1969*, McGraw-Hill, New York, 1969.

[9]Anon., "Evaluation of STOL Microwave Facility Performance Requirements," FAA Standards Development Branch, National Flight Inspection Div., Flight Standards Service, Washington, D. C., Jan. 1972.

[10]Benner, M. S., Sawyer, R. H. and McLaughlin, M. D., "A Fixed-Base Simulation Study of Two STOL Aircraft Flying Curved Descending Instrument Approach Paths," TN D-7298, NASA, 1973.

[11]McMurty, T. C., Gee, S. W., and Barber, M. R., "A Flight Investigation of Curved Steep Approach Profiles for STOL Operations," STOL Technology Conference, Oct. 17-19, 1972, NASA Ames Research Center, Moffett Field, Calif.

[12]Anon., "A New Guidance System for Approach and Landing," RTCA SC-117, RTCA DO-148, Dec. 1970.

[13]Anon., "Automatic Landing System," Advisory Circular 20-57A, Federal Aviation Agency, Washington, D.C., Jan. 12, 1971.

[14]Anon., "Criteria for Approving Category I and Category II Landing Minima for FAR 121 Operations," Advisory Circular 120-29, Federal Aviation Agency, Washington, D. C., Sept. 25, 1970.

Downloaded by UNIVERSITY OF CALIFORNIA - DAVIS on February 9, 2015 | http://arc.aiaa.org | DOI: 10.2514/3.58644

From the AIAA Progress in Astronautics and Aeronautics Series . . .

AEROACOUSTICS: FAN, STOL, AND BOUNDARY LAYER NOISE; SONIC BOOM; AEROACOUSTIC INSTRUMENTATION—v. 38

Edited by Henry T. Nagamatsu, General Electric Research and Development Center; Jack V. O'Keefe, The Boeing Company; and Ira R. Schwartz, NASA Ames Development Center
A companion to Aeroacoustics: Jet and Combustion Noise; Duct Acoustics, volume 37 in the series.

Twenty-nine papers, with summaries of panel discussions, comprise this volume, covering fan noise, STOL and rotor noise, acoustics of boundary layers and structural response, broadband noise generation, airfoil-wake interactions, blade spacing, supersonic fans, and inlet geometry. Studies of STOL and rotor noise cover mechanisms and prediction, suppression, spectral trends, and an engine-over-the-wing concept. Structural phenomena include panel response, high-temperature fatigue, and reentry vehicle loads, and boundary layer studies examine attached and separated turbulent pressure fluctuations, supersonic and hypersonic.

Sonic boom studies examine high-altitude overpressure, space shuttle boom, a low-boom supersonic transport, shock wave distortion, nonlinear acoustics, and far-field effects. Instrumentation includes directional microphone, jet flow source location, various sensors, shear flow measurement, laser velocimeters, and comparisons of wind tunnel and flight test data.

509 pp. 6 x 9, illus. $19.00 Mem. $30.00 List

TO ORDER WRITE: Publications Dept., AIAA, 1290 Avenue of the Americas, New York, N. Y. 10019